STUDIA UBB CHEMIA, LXIV, 3, 2019 (p. 99-109)
(RECOMMENDED CITATION)
DOI:10.24193/subbchem.2019.3.08

MORPHO-STRUCTURAL AND PHOTOCATALYTIC PROPERTIES OF SnO_2 NANOPARTICLES

MARIA ŞTEFAN[a,*], OVIDIU PANA[a], CRISTIAN LEOSTEAN[a], ADRIANA POPA[a], DANA TOLOMAN[a], SERGIU MACAVEI[a], DIANA LAZAR[a], LUCIAN BARBU-TUDORAN[a]

ABSTRACT. SnO_2 nanoparticles were successfully synthesized by precipitation method, in the presence of hexadecyltrimethyl ammonium bromide (CTAB) and polyethylene glycol 600 (PEG 600) as surfactants. The obtained SnO_2 nanoparticles were characterized by X-ray diffraction (XRD), porosity and surface area measurements (BET), high resolution transmission electron microscopy (HRTEM), X-ray photoelectron spectroscopy (XPS). Also, photocatalytic properties toward degradation of Rhodamine B (RhB) were investigated. It was found that morpho-structural properties are influenced by the preparative conditions of doped SnO_2 nanoparticles.

Keywords: *SnO_2; nanoparticles; photocatalytic properties*

INTRODUCTION

Wastewater decontamination is a stringent requirement in the research field of environmental protection [1-4]. Utilization of green and cheap technologies has been considered a convenient solution to complete degradation of organic pollutants released from industry [5-8].

Photocatalysis is an advanced oxidation method used for removing organic contaminants such as organic dyes, antibiotics, etc from aquatic system. Generally, semiconductor materials namely metal oxides have been employed for the photo-degradation of organic contaminants [9-10]. Among various oxides SnO_2 is one of the most popular and promising materials in wide range of applications such as gas sensing, photocatalytic applications, solar cells, lithium-ion batteries, because of its high stability, non-toxicity, eco-friendly and low cost [11-15].

[a] *National Institute for Research and Development of Isotopic and Molecular Technologies, 67-103 Donath Str., RO-400293 Cluj-Napoca, Romania.*
** Corresponding author: mstefan@itim-cj.ro*

The obtaining of nanoparticles with predetermined size and shape represents the target of materials chemistry [16-19]. The morpho-structural properties of oxide nanoparticles can be controlled by addition in synthesis procedure of various surfactants [20, 21]. It is known that organic surrounding environment and surface passivation can provide stability and additional functionality to the nanoparticles. In the present work we report influence of different surfactants on morpho-stuctural properties of SnO_2 nanoparticles. Also, the photocatalytic properties of samples for degradation of rhodamine B (RB) were evaluated.

RESULTS AND DISCUSSION

Generally, the properties of nanoparticles can be controlled by a rigorous modification of experimental parameters. SnO_2 nanoparticles were obtained by precipitation method in the presence of different surfactants. The general chemical equations for obtaining of SnO_2 nanoparticles are:

$$SnCl_2 + 2NaOH \rightarrow Sn(OH)_2 + 2NaCl \quad (1)$$
$$Sn(OH)_2 \rightarrow SnO + H_2O \quad (2)$$
$$SnO+1/2O_2 \rightarrow SnO_2 \quad (3)$$

The crystalline structure of the obtained nanoparticles was evidenced by X-ray diffraction. Figure 1 shows the diffraction patterns and corresponding indexation of S1, S2 and S3 samples. The diffraction peaks are sharp and strong indicating the good crystallinity of the samples. All of them together with corresponding reflection planes can be indexed to tetragonal SnO_2 nanoparticles (WWW-MINCRYST, CASSITERITE-779). No other peaks were observed such as Sn or any other Sn based oxide, indicating the high purity of the samples.

Using the Scherer formula, along (110) diffraction lines, the average crystallite sizes of all the samples have been determined. The calculated values are 10.8 nm (S1), 11.3 nm (S2) and 11.5 nm (S3), respectively. The addition of surfactants in the synthesis procedure for the obtaining of SnO_2 nanoparticles seems to favor the increase of the crystallite sizes.

Figure 2 shows the transmission electron microscopy (TEM) images of the SnO_2 nanoparticles obtained with/ without surfactants. It can be seen that nanoparticles consist of small particles with tetrahedral shape with diameters around 11 nm, showing a strong tendency toward agglomeration. It can be seen that the addition of surfactants slightly changes the morphology of SnO_2 nanoparticles.

The representative high-resolution TEM (HRTEM) images are given in figure 3. Lattice fringes are clearly visible in images revealing the crystalline nature of nanoparticles. Based on the Fourier analysis of this image, to crystalline planes of SnO_2 (110) was identified.

For qualitative analysis of samples, the following XPS core-level lines were recorded: Sn 3*d*, O 1*s* and C 1*s*. The C 1s line associated to C-C or C-H bindings positioned at 284.6 eV was used for spectra calibration. As an example, the XPS spectrum together with the corresponding deconvolutions of Sn 3*d* core-levels for sample S3 is shown in figure 4.

The restrictions used for fitting the spectrum refer to the relation between integral intensities of the doublet components $I_{(5/2)} = (2/3)I_{(3/2)}$ and doublet separation considered as 8.4 eV. The observed position of 488.0 eV for Sn 3*d* (5/2) and 496.4 eV for Sn 3*d* (3/2) is characteristic to Sn^{4+} oxidation state. Two shake-up satellites positioned at 491.5 eV and 499.9 eV were also used in the deconvolution process. Samples S1 and S2 show similar Sn 3*d* spectra, characteristic to Sn^{4+} oxidation state.

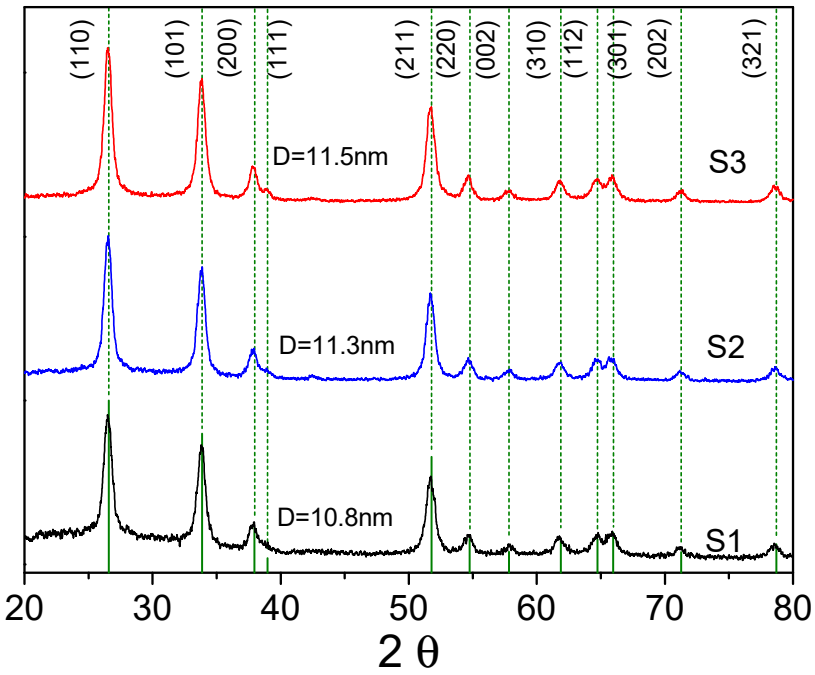

Figure 1. Diffraction patterns and corresponding indexation of S1(SnO_2), S2 (SnO_2-CTAB) and S3(SnO_2-PEG600) nanoparticles

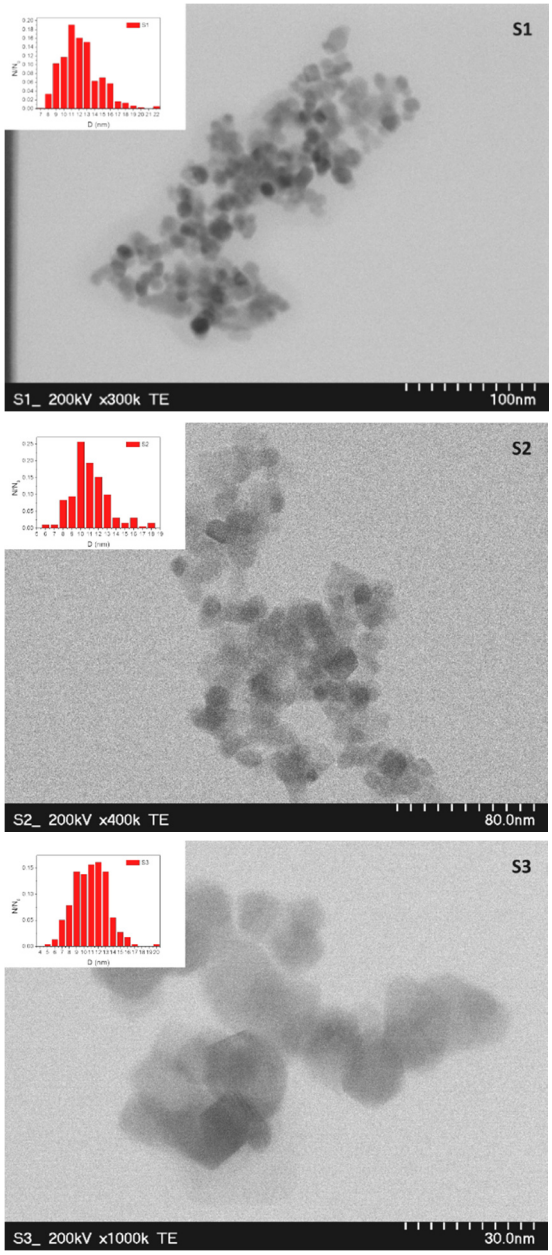

Figure 2. TEM images of SnO_2 nanoparticles obtained with different surfactants S1-SnO_2, S2-SnO_2-CTAB, S3- SnO_2-PEG600

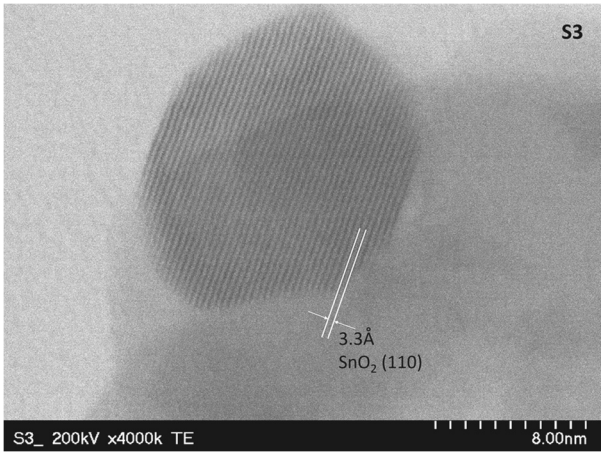

Figure 3. HRTEM image corresponding to S3(SnO_2-PEG600) sample

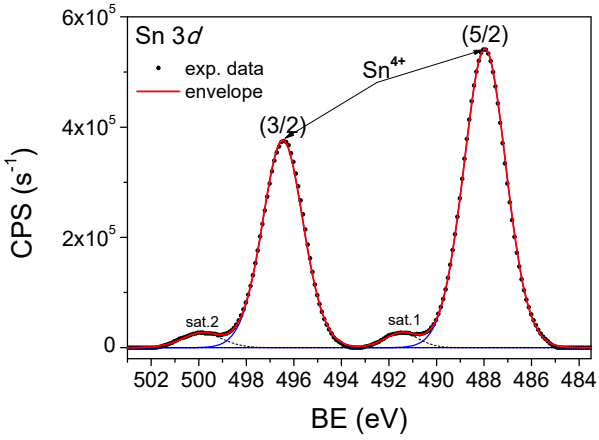

Figure 4. XPS spectrum of Sn 3*d* core-levels together with the corresponding deconvolutions in case of S3 (SnO_2-PEG600) sample.

The N_2 adsorption–desorption isotherms and corresponding pore size distribution of SnO_2 nanoparticles are shown in Figure 5 (a, b). The results indicate that for all samples the isotherms are of types IV with hysteresis loop on the desorption branch, sustaining the mesoporous structure of samples. Also, the pore size distribution shows mean diameter of 80 Å that confirmed the presence of mesopores. Other data such as BET surface area, pores volumes were also calculated and are given in Table 1.

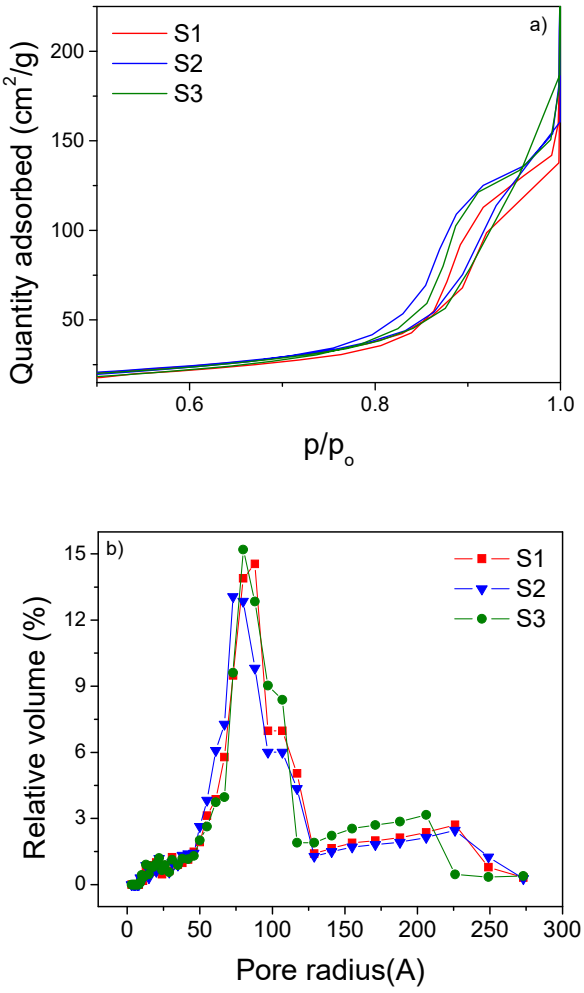

Figure 5. N_2 adsorbtion-desorption isotherms (a) and corresponding pore size distribution; (b) of nanoparticles: S1(SnO_2), S2(SnO_2-CTAB)and S3(SnO_2-PEG600)

The BET surface area of SnO_2 nanoparticles prepared with/without surfactants varies from 45.29 - 47.16 m^2/g, depending on surfactant type. The addition of CTAB seems to have no effect on surface area. Also, the pore volume was found to increase for sample with PEG 600. This behavior is due to the partial/total removing of surfactants in the calcinations process.

Table1. Surface area and pores characteristic of SnO_2 nanoparticles with/without surfactants

Sample	BET surface area (m^2/g)	Pore volume (cm^3/g)
S1(SnO_2)	47.16	0.24
S2 (SnO_2-CTAB)	47.16	0.23
S3(SnO_2-PEG600)	45.29	0.25

The photocatalytic activity of the synthesized samples was estimated by examining the degradation of Rhodamine B (RhB) pollutant. Prior to the photocatalytic process, the RhB adsobtion on SnO_2 nanoparticles surface, in the dark was tested. It was observed that the adsorption-desorption equilibrium was reach after 30min. All samples present similar adsorption, only a small amount of RhB molecules being adsorbed at the nanoparticles surface. After the equilibrium was reached, the RhB solution containing the nanoparticles was irradiated by visible light. The changes in intensity of the UV-VIS absorption peak of RhB situated at 554 nm as a function of irradiation time was monitored.

As an example, figure 6 presents the evolution of RhB absorption peak intensity in the presence of S1 sample at different irradiation time intervals. Based on the absorption changes, the photocatalytic activity was calculated. The photocatalytic activity of RhB in the presence of S1, S2 and S3 samples is shown in figure 7. After 180 min of visible light irradiation, only 19-24% of the RhB dye was degraded by S3 and S2 sample, whereas 98% of the RhB dye was degraded by S1 sample.

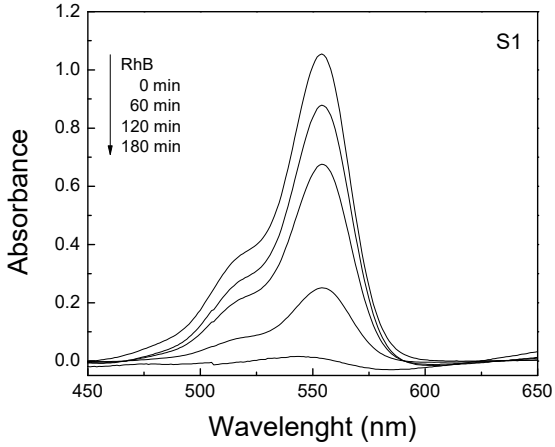

Figure 6. UV–vis absorption spectra of RhB aqueous solution in the presence of S1(SnO_2) sample at different irradiation time interval

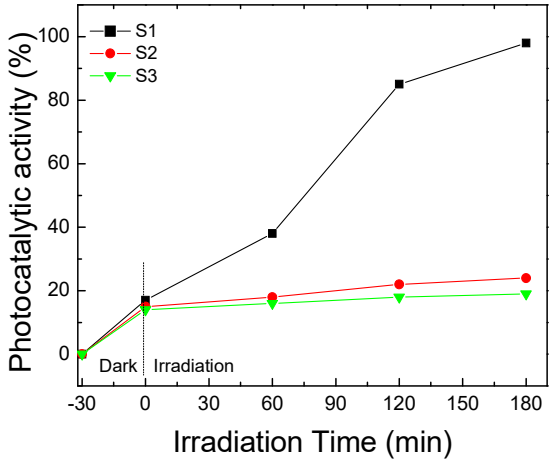

Figure 7. Photocatalytic degradation of RhB in the presence of S1(SnO_2), S2(SnO_2-CTAB) and S3(SnO_2-PEG600) nanoparticles

Since the photocatalytic process takes place mainly on the nanoparticles surface, the surface-to-volume ratio and the pore size are important parameters involved in pollutant degradation. Seems that the surfactants presence on the surface of SnO_2 inhibit the photocatalytic process.

EXPERIMENTAL SECTION

Materials

The chemical reagents used for the preparation of SnO_2 nanoparticles are: tin chloride $SnCl_2x2H_2O$ (for synthesis, Merck), sodium hydroxide (98% Alpha Aesar), hexadecyltrimethyl ammonium bromide $C_{19}H_{42}NBr$-CTAB (99%, Sigma) and polyethylene glycol 600 (PEG 600).

All chemicals are analytical grade without further purification and were used as received.

Sample preparation

The SnO_2 nanoparticles were obtained by chemical precipitation starting from aqueous solution of tin chloride dihydrate-$SnCl_2x2H_2O$ and sodium hydroxide-NaOH in the presence of different surfactants. In the synthesis procedure, 3.2 mM of $SnCl_2x2H_2O$ were dissolved in 100 ml water and then 100 ml NaOH solution (3.2 mM) was added drop wise in the solution. Different surfactants such as CTAB and PEG 600 were added into mixture.

After the addition of NaOH was finished, the reaction was kept 4h under vigorous stirring. The as prepared SnO_2 nanoparticles were separated by centrifugation and washed with water and ethanol (1:1 v/v) for several times to remove the excess of reactants and then dried at 65 ^{0}C, in air. Finally, the dried samples were thermally treated for 2 h at 500^{0}C in furnace, at a rate of 10^{0}C/min, in order to get the crystalline SnO_2 nanoparticles. In order to evidenced the influence of organic additive on properties of the SnO_2 nanoparticles different samples were prepared as follows: S1-SnO_2, S2-SnO_2 -CTAB, S3- SnO_2 -PEG600.

Samples characterization

The crystalline structures were evidenced by X-ray diffraction (XRD), recorded by using a Bruker D8 Advance X-ray diffractometer set-up, at 40 kV and 40 mA equipped with a germanium monochromator in the incident beam. The X-ray diffraction patterns were collected in a step-scanning mode with steps of $\Delta\theta = 0.02°$ using Cu Kα1 radiation ($\lambda = 1.54056$ Å) in the 2θ range 10^o-80^o. Pure silicon powder was used as standard for instrument broadening correction.

The morphology of the composite nanoparticles was determined by transmission electron microscopy (TEM) and high resolution TEM (HRTEM). The TEM measurements were performed with Hitachi SU8230 Transmission Electron Microscope equipped with a cold field emission gun. The powders were dispersed in ethanol, with a BANDELIN SONOREX homogenizer and deposited on 400 meshes copper grid, which was coated with carbon film. The HRTEM images were collected with Hitachi H9000NAR transmission electron microscope. The qualitative and quantitative compositions of samples were investigated by using X-Ray Photoelectron Spectroscopy (XPS) assisted by Ar ions etching. The XPS spectra were recorded by using a SPECS spectrometer working with Al anode (1486.6 eV) as X-rays source. Each sample was subject of several Ar ions etchings until the XPS spectra remained unchanged in shape and intensity. At this stage the XPS spectra reflect the real composition of samples. In order to avoid artificial reduction of different oxidation stats of elements the etching was performed by using Ar ions accelerated at a maximum 1000 V voltage with a filament current of 10 mA.

Surface area measurements were performed with a Micromeritics TriStar II 3020 instrument, nitrogen adsorption at 77 K. All samples were degassed at 150 ^{o}C for 24 h in nitrogen flow) Brunauer - Emmett – Teller (BET) analysis and BJH analysis (Baret, Joyner, and Halenda method) was used to determine area and volume of the mezo and macropores using adsorption and desorption techniques.

The photocatalytic activity of the SnO_2 nanoparticles was evaluated by photodegradation of Rhodamine B (RhB) in a Laboratory-Visible-Reactor system with a 400 W halogen lamp (Osram) which emits in visible range. The irradiation was performed under ultrasonically stirring. The catalyst (12 mg) was suspended in aqueous solution of RhB (1.0×10^{-5} mol L^{-1}, 8 mL) and then the mixture was stirred in the dark to achieve the adsorption equilibrium on the catalyst surface. Each degradation experiment was continuously conducted for 180 min. 3.5 mL of the mixed suspension was extracted at given intervals of illumination and separated with a magnet to remove the photocatalysts.

Finally, the clear supernatant was measured by recording the maximum absorbance of RhB at 554 nm. To separate the nanocomposites from the solution after the photodegradation of RhB a magnet was used. The photocatalyst was recycled three times and each experiment cycle used a fresh RhB solution under the same experimental conditions.

Photocatalytic activity is calculated using the following equation:

$$\text{Photocatalytic activity} = \frac{A}{A_0} \text{ x } 100 \quad (4)$$

where, A_0 and A represent the initial and the changed absorbance of RhB at 553 nm, respectively.

CONCLUSIONS

SnO_2 nanoparticles were prepared in the presence of different surfactants: hexadecyltrimethyl ammonium bromide (CTAB) and polyethylene glycol 600 (PEG 600). XRD investigations evidenced the crystalline nature of samples. The formation of crystalline nanoparticles with polyhedral shape was confirmed by TEM/HRTEM. The surface area measurements evidenced that SnO_2 nanoparticles have mesoporous structure with average pore size 80 nm. The surface area of nanoparticles varies from 45.29 - 47.16 m^2/g, depending on surfactant type. XPS investigations show the oxidation state Sn^{4+} in the samples. The photocatalytic measurements reveal that SnO_2 nanoparticles have photocatalytic efficiency toward the degradation of RhB solution. The presence of surfactants inhibits the photocatalytic response.

ACKNOWLEDGEMENTS

The authors would like to express appreciation to the Romanian Ministry of Research and Innovation for the financial support through Project PN19 35 02 03 (Core Program).

REFERENCES

1. Z.L. Wang, W.Z. Wu, *Angew. Chem*. **2012**, *51*, 11700.
2. K. Sornalingam, A. McDonagh, J. L Zhou, M.A.H. Johir, M.B. Ahmed, *Sci. Tot. Env.* **2018**, *610*, 521.
3. H.J. Zhang, G.H. Chen, D.W. Bahnemann, Photoelectrocatalytic materials for environmental applications, *J. Mat. Chem*., **2009**, *19*, 5089.
4. K. Prakash, P.S. Kumar, K. Saravanakumar, S. Karuthapandian, *J. Exp. Nanosci.*, **2016**,1, 1.
5. S. Zang, M. Zeng, J. X. Li, *J. Mater. Chem. A*, **2014**, *2*, 4391.
6. M. Abdullah, A. Hamdi, M. Sillanpaa, *J. Mater. Sci*., **2014**, *49*, 5151.
7. Q. Du, G. Lu, *Appl. Surf. Sci.*, **2014**, *305*, 235.
8. C. Tang, V. Chen, *Water. Res*., **2004**, *38*, 2775.
9. P.S. Kumar, M. Selvakumar, P. Bhagabati, et al, *RSC Adv*., **2014**, *4*, 32977.
10. R. Zhang, H. Wu, D.D. Lin, W. Pan, *J. Am. Ceram. Soc*., **2009**, 92, 2463.
11. A. Ahmed, M.N. Siddique, U. Alam, T. Ali, P. Tripathi, *Appl. Surf. Sci*., **2019**, 463, 976.
12. M.S. Park, G.X. Wang, Y.M. Kang, D. Wexler, S.X. Dou, H.K. Liu, *Angew. Chem*. **2007**,119764–767
13. A. Borhaninia, A. Nikfarjam, N. Salehifar, *Trans. Nonferrous Met. Soc. China,* **2017**, 27, 1777.
14. Y. Li, Q. Yang, Z. Wang, G. Wang, B. Zhang, Q. Zhang, D. Yang, *Inorg. Chem. Front.,* **2018**, ***5***, 3005.
15. R. Mani, K. Vivekanandan, K. Vallalperuman, *J. Mater. Sci. Mater. Electron*., **2017**, *28*, 4396.
16. K. Prakash, P. Senthil Kumar, S. Pandiaraj, K. Saravanakumar, S. Karuthapandian, *J. Exp. Nanosci.,* **2016**, *11*, 1138.
17. S. Shi, D. Gao, Q. Xu, Z. Yang, D. Xue, *RSC Adv*., **2014**, *4*, 45467.
18. B. Babu, A.N. Kadam, G.T. Rao, S.W. Lee, C. Byon, J. Shim, *J. Lumin*., **2018**,*195*, 283.
19. K. Anandan, V. Rajendran, *Superlattices Microstruct*. **2015**, *85*, 185.
20. A. Bhattacharjee, M. Ahmaruzzaman, T. Sinha, *RSC Adv*., **2014**, *4*, 51418.
21. H. Choi, E. Stathatos, D. D. Dionysiou, *Topics in Catal.*, **2007**, *44*, 513.